Spider Intermodular Connection: An innovative connection solution for steel modular buildings

Ricardo Aguayo[*], Jorge Conde[b], Ana Francisca Santos[a] , Luís Simões da Silva[a], David Andrade[a], Filip Ljubinković[a], Sree Sabari[a]

[a] University of Coimbra, ISISE, ARISE, Department of Civil Engineering, Coimbra, Portugal, Universidade de Coimbra
[b] Universidad Politécnica de Madrid, Departamento de Física y Estructuras de Edificación, Av. Juan de Herrera, 4, 28040 Madrid, Spain. https://orcid.org/0000-0002-5633-1170

[*] Author for contact. Tel.: +351 929432326; E-mail: aguayoortega@uc.pt

Abstract: Modular construction systems face significant challenges in ensuring structural continuity, particularly at inter-module joints where connection performance governs both local behaviour and global response. Within the framework of the R2U project, which fosters the industrialisation of modular construction in Europe, this study introduces the Spider inter-module connector, a prototype specifically designed to guarantee vertical continuity in stacked 3D steel modules with square hollow sections. A comprehensive full-scale experimental campaign was carried out to characterise the connector's tensile response. Complementary finite element analyses were developed in Abaqus and calibrated against the experimental results, demonstrating the role of the horizontal preload levels and internal blocking plates support conditions exert a decisive influence on the connection's performance.

1. Introduction

The modular construction system has emerged as a promising solution for building facilities. However, the structural performance of modular buildings is strongly conditioned by the local response of intermodular connections (IMCs), which act as links ensuring continuity of load paths across modules. The limited space available for connection detailing constrains the structural performance. Different studies have shown that the stiffness and energy dissipation capacity of IMCs directly influence both the local and global behaviour under static and dynamic conditions **[1], [2]**. Recent reviews have systematically classified the modular connection typologies **[3],** understanding their performance requirements **[4]**, and highlighting persisting limitations such as slips, gap opening, and insufficient ductility in conventional bolted system **[5]**. **Fig. 1** describes 5 existing typologies of connections reported in the literature, together with their description, advantages and disadvantages**[6], [7], [8], [9]**. Parametric studies have been

widely used to examine how local connection parameters influence the lateral behaviour, vibration response, and collapse capacity of modular buildings **[10]**. Shin, et al. **[11]** proposed a semi-rigid post-tensioned inter-module connection with a central shear key and reported that applying approximately a preload of around 10% of the axial column capacity was sufficient to prevent slip and ensure stable seismic performance. A novel HDR + SMA hybrid connection enhances ductility, energy dissipation, and reusability of modular steel buildings, providing more sustainable and resilient solutions **[12]**. Lee et al. **[9]** proposed a bolt-free preloaded system with high–strength rods and developed a combined analytical–numerical method to determine the minimum preload required to avoid slip and gap opening, regarding the beam's stiffness and module self-weight. Rajanayagam, et al. **[13]** showed that "end plates" inside of column's module (plates welded and integrated within the column's module manufacturing) strongly affect the tensile response due to the lack of welding penetration inside the column's module. Kujawa et al. **[14]** demonstrated that post-tensioned inter-module connections, when subjected to appropriate preload levels, can achieve high stiffness and strength while minimising slip and enhancing overall structural robustness. Peng et al. **[15]** showed that applying the *strong-column weak-beam* (SCWB) concept enables modular buildings to achieve global rather than local failures, while adequate preload in the connections further enhances slip resistance and stiffness, ensuring safer and more robust seismic performance. Liew and Chua **[16]** developed plug-in modular connections for high-rise buildings that improve load transfer, ductility, and energy dissipation, while reducing slip and gap opening compared with conventional bolted systems.

The development of intermodular connections in the context of *R2U -Technologies* project (focused on modular building solutions to construction industry), primarily the Long Bolt **[17]** and Spider **[18]** inter-modular joints for steel prefabricated modules, represents a major advancement, offering prefabricated solutions that combine preloading, tolerance control, and efficient assembly for stacked modular buildings. In particular, the Spider connector employs a horizontal and vertical non-conventional preload friction system, combined with an internal mechanical accommodation for tolerances, making its design unique within its typology. This paper presents the experimental campaign and preliminary numerical validation of the Spider connector in tension developed at University of Coimbra within the scope of the R2U Project

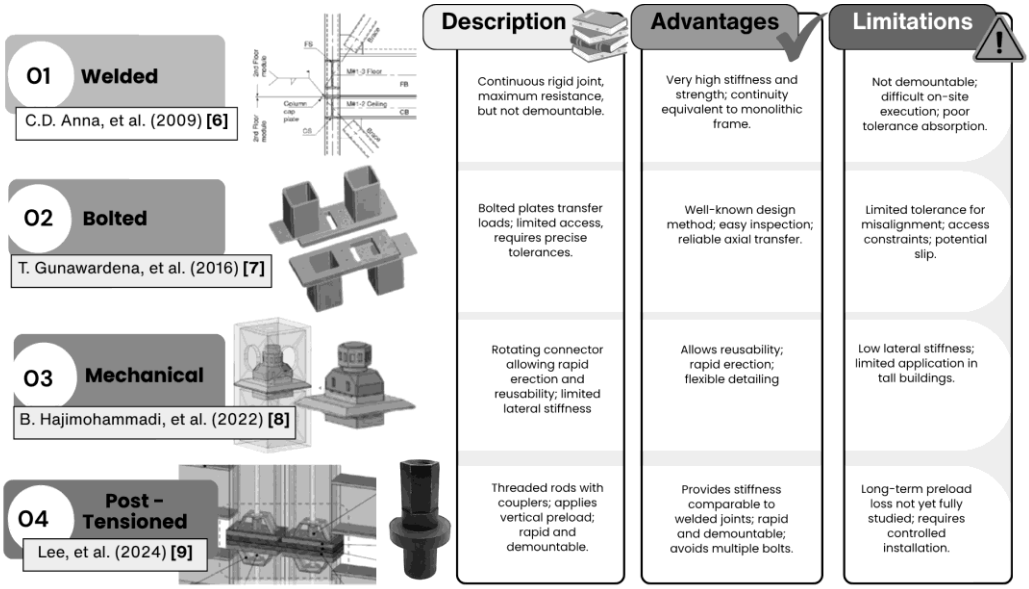

Fig. 1 .- Modular Joint system already presented in Literature Review

2. Intermodular Spider Connector: Description

The Spider connector is an innovative modular joint system engineered to facilitate efficient assembly and disassembly in steel modular buildings. It is specially designed to allow the stacking of finished modules with tubular column sections, in which the access is restricted to the top of the module. **Fig. 2** shown the spider connector schematic in the modular building system with component identification and summary table.

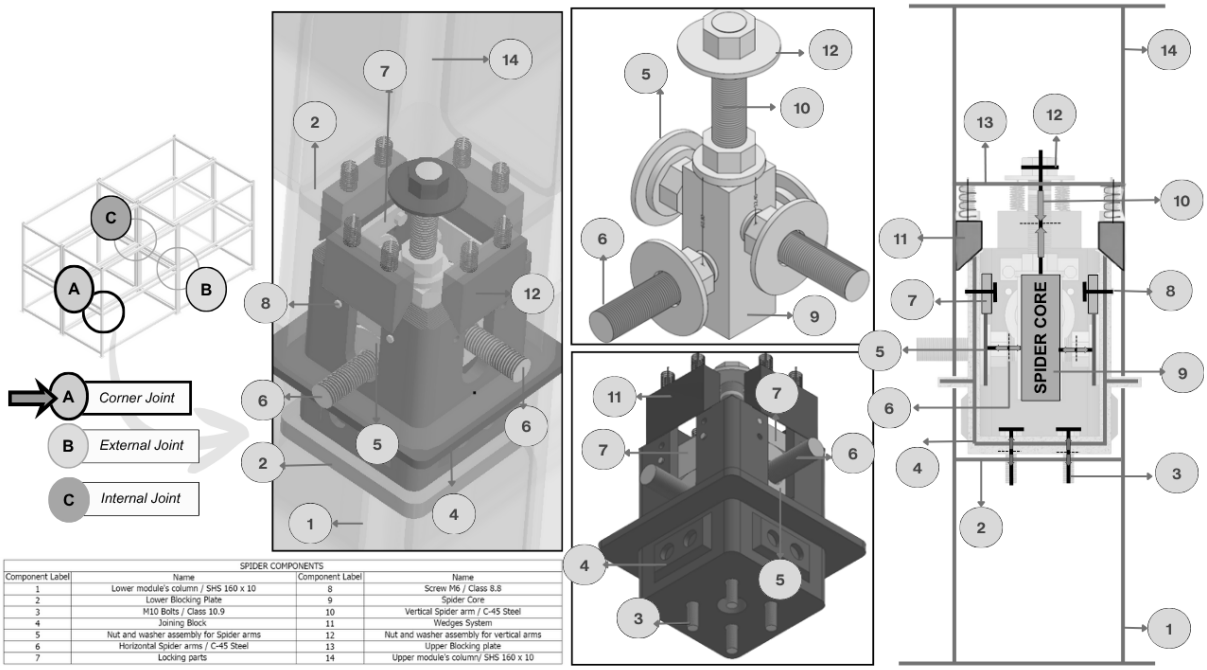

SPIDER COMPONENTS

Component Label	Name	Component Label	Name
1	Lower module's column / SHS 160 x 10	8	Screw M6 / Class 8.8
2	Lower Blocking Plate	9	Spider Core
3	M10 Bolts / Class 10.9	10	Vertical Spider arm / C-45 Steel
4	Joining Block	11	Wedges System
5	Nut and washer assembly for Spider arms	12	Nut and washer assembly for vertical arms
6	Horizontal Spider arms / C-45 Steel	13	Upper Blocking plate
7	Locking parts	14	Upper module's column/ SHS 160 x 10

Fig. 2 Spider connector – Modular connection, corner typology

The core of the system comprises a solid steel core (component **9** in **Fig. 2**) from which four horizontal (component **5** in **Fig. 2**) and one vertical arm extend (component **10** in **Fig. 2**), all based on M20 threaded rods. C45 steel (with a nominal yield strength of 600 MPa and tensile strength of 400 MPa) was used for manufacturing the threaded rods. Each horizontal rod features opposing threads: one end is embedded within the central core, while the opposite end is externally preloaded using a washer–nut assembly (component **5** in **Fig. 2**). This mechanism induces a compressive preload along the horizontal axis of the spider, clamping the internal surfaces of the joining block (component **4** in **Fig. 2**) against the Spider's core (component **9** in **Fig. 2**) and establishing a stable, expansion-based innovative connection for modular joint systems.

The applied horizontal preload allows the Spider connector to mobilise frictional resistance at the interface between the washers (component **5** in **Fig. 2**) and the internal faces of the joining block. Once the maximum frictional capacity is exceeded, vertical load transfer is safeguarded by dedicated locking components (component **7** in **Fig. 2**) acting as shear-transfer mechanisms. These locking plates provide a secondary stiffness, ensuring reliable vertical force transmission and preventing slippage in the event of frictional degradation or loss.

The joining block (component **4** in **Fig. 2**) acts as a combined tension – shear transfer mechanism. At the top, its serrated edges engage with wedge components (component **11** in **Fig. 2**) to secure load transfer in shear. This system also accommodates construction-induced eccentricities of up to +10 mm. At the base, tensile forces are transmitted through four M10, class 10.9 bolts (component **3** in **Fig. 2**), with a reduced preload condition. These bolts are threaded exclusively into the pre-tapped holes of the lower blocking plate.

3. Experimental Campaign Summary

The experimental campaign was designed to evaluate the structural performance of modular prototype connections. The test specimen comprised two SHS 160 x 10 columns, each 400 mm in length, joined by a Spider connector. The total assembled height of the configuration was 868 mm. The connector was subjected to axial tension using a servo-hydraulic testing system with a maximum capacity of 500 kN. The specimen was directly mounted over the reaction frame as illustrated **Fig. 3**. The objective was to characterise its load-bearing capacity, initial stiffness, ductility, and failure mechanisms. The specimen is presented in **Fig. 3** with its respective LVDT instrumentation used for characterisation of axial response.

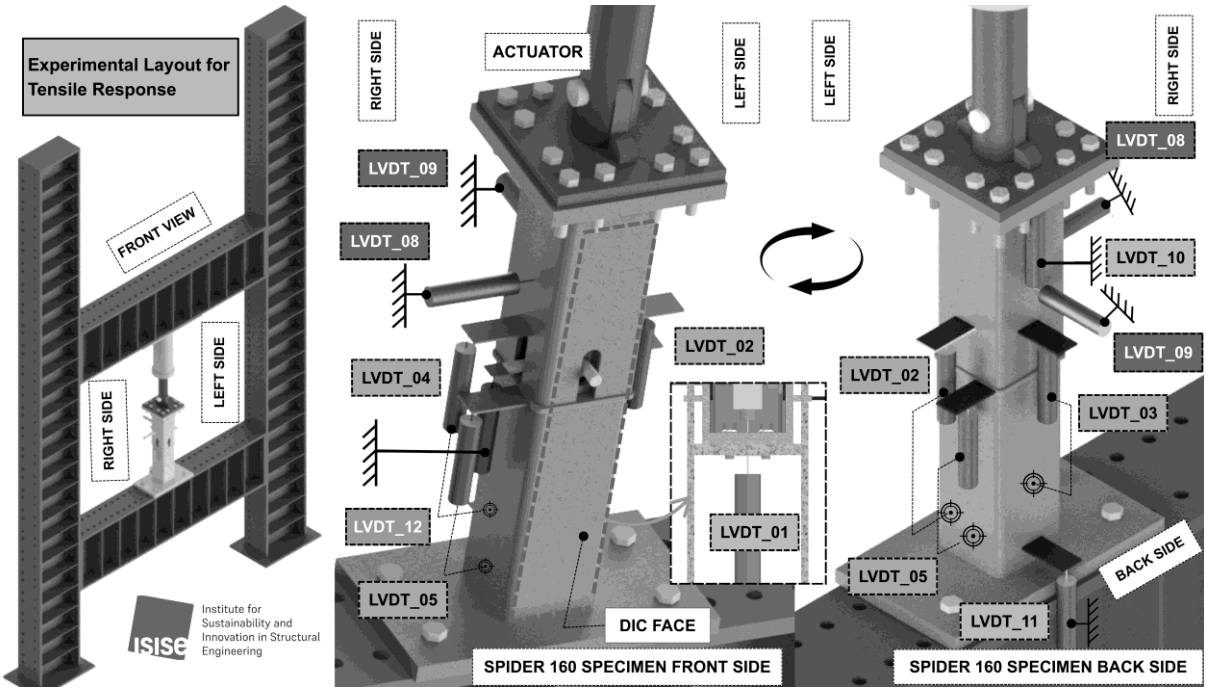

Fig. 3 .- Experimental Layout of Spider - 160 under tension.

Fig. 4 summarises the results of the experimental campaign. The force–displacement response of the Spider connector under axial tension, measured directly by LVDT_01, is presented in **Fig. 4a** LVDT_01 was strategically positioned in direct contact with the connector's central core through a 26 mm access hole (see **Fig. 3**). The curve shows an initial vertical preload of approximately 15 kN, followed by a linear elastic response up to 53 kN. Beyond this point, progressive engagement of the locking components introduces post-yield stiffness, marking the transition to the inelastic regime. The system exhibited notable ductility, reaching a displacement of 7 mm at a peak load of approximately 75 kN, due to bearing of locking plates (see **Fig. 4b**).

The same trends were observed in the readings of LVDT_12 (located at the external horizontal arms of the spider) in comparison with the LVDT_01 (see **Fig. 4a)**, confirming the rigid-body behaviour of the Spider connector. Additional curve was develop regarding the DIC point measured at the front spide horizontal arm (see **Fig. 4a**). Additional displacements were recorded at the specimen's top and bottom using LVDT_10 (Upper Column) and LVDT_11 (Bottom Column), as reported in **Fig. 4d** in comparison with DIC Data. In-plane and out-of-plane eccentricities were also monitored with LVDT_08 and LVDT_09 (see **Fig. 4c)**, reaching maximum values of 0.7 mm (0.8% of the specimen height) and 0.4 mm (0.5% of the specimen height), respectively. These eccentricities have a negligible influence on the global structural response, as they remained below 2% of the total specimen's height.

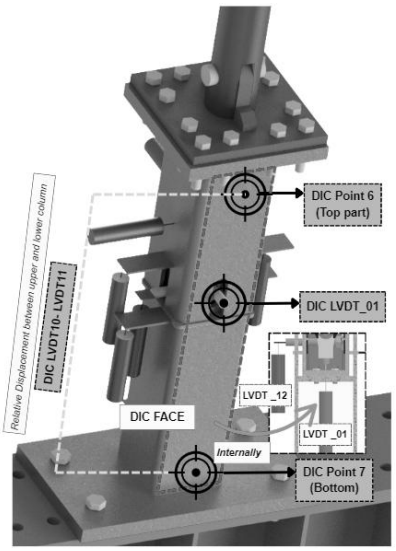

a) DIC Point and LVDTs

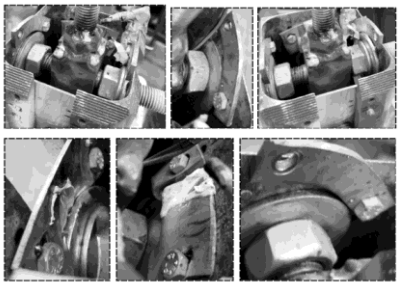

b) Spider's mode of failure

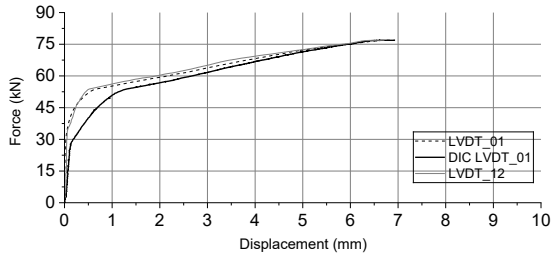

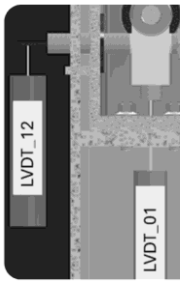

c) Internal measurement with LVDT_01 and LVDT_12

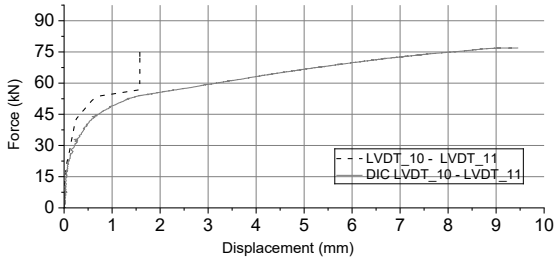

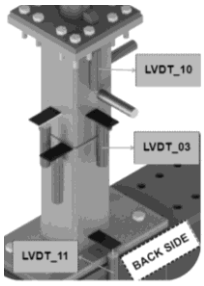

d) External Calibration with LVDT_10 and LVDT_11

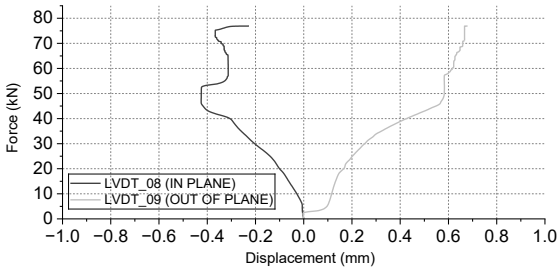

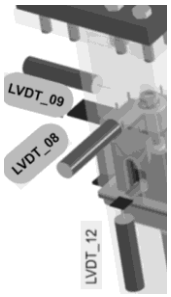

e) Eccentricity control and positioning within the layout

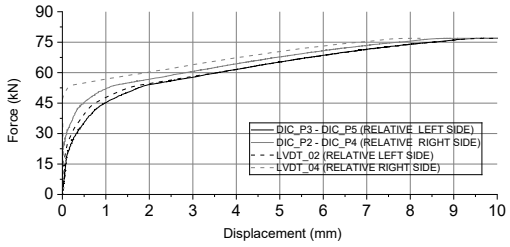

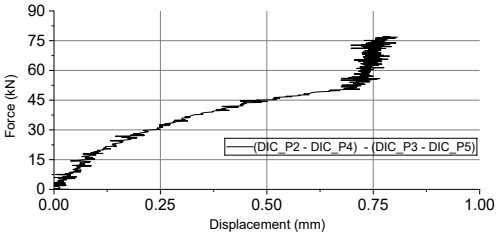

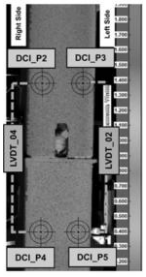

f) DIC Data benchmark data and specimen inclination.

Fig. 4 .- Experimental Campaing Summary data.

Additional displacement data were collected in the joint zone through LVDT_02, LVDT_03, and LVDT_04 to characterise the local response. The measurements indicated a slight inclination of the specimen during the tensile test, with the right side showing uplift relative to the left. To double-check this observation, Digital Image Correlation (DIC) analysis was performed with particular focus on the connection zone. **Fig. 4f** confirms a maximum uplift of 0.70 mm between the right and left sides; after reaching 50 kN, both sides remained aligned. This observation suggests that a geometric condition is responsible for the slight asymmetry and should be further investigated through finite element modelling.

4. Numerical simulations

4.1 Numerical Modelling Strategy

A detailed preliminary FE study was carried out to replicate the tensile response of the Spider connector. As the system involves multiple nonlinear effects, including preloaded bolts in different directions, internal confinement, construction tolerances, and complex contact interfaces, a progressive, multi-step modelling strategy was adopted to properly understand the structural response. **Fig. 6** details the different models and explains the outcomes and limitations imposed. This approach allowed the role of individual components to be isolated, ensuring stable convergence, and progressively reproduced the full assembly behaviour. The analysis was performed in Abaqus/Standard using a Static General procedure, which provided greater accuracy but also introduced potential convergence challenges due to complex contact interactions. The General Contact definition allows the capture of relative slip and gap formation across the interfaces. A hybrid mesh was employed, combining C10D3R tetrahedral elements for the Spider's steel core (due to its complex geometry) and C3D8R hexahedral elements for the remaining parts. The static analysis was divided into two stages: (i) application of preload and (ii) tensile loading, both considering geometric nonlinearities.

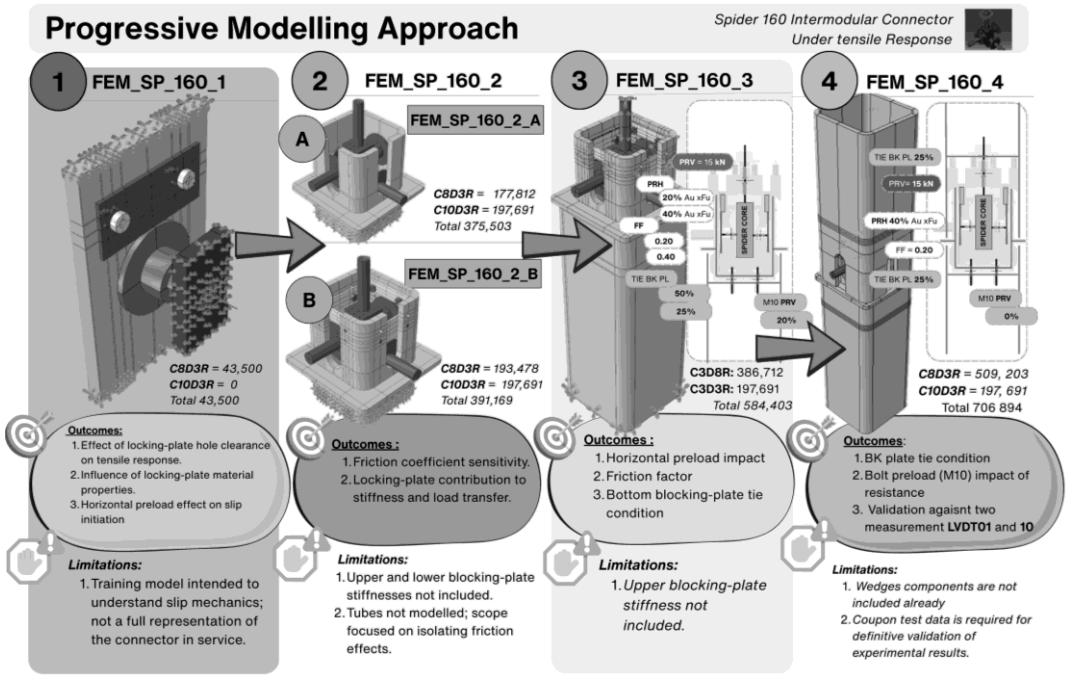

Fig. 5 : Progressive Modelling Approach methodology

Geometric imperfections were not considered in the numerical models. For this initial stage, nominal material properties were adopted for the calibration of the FEM simulations. A friction coefficient of 0.20 was assumed for the final model, reflecting the untreated surface condition of the joining block with ground steel; the influence of this parameter was also investigated in sensitivity analyses.

Material behaviour for carbon steel was defined using the characterisation proposed by Yun and Gardner **[19]**, incorporating true stress–strain curves. Horizontal preload levels were evaluated between 20% and 40% of axial tensile rods strength, while tie conditions were varied between 25% and 50% to approximate the contribution of the blocking plate weld, accounting for the possible lack of full penetration due internal space limitation

5. Analysis of Results

The validation process of the Spider connector under tensile loading is illustrated in **Fig. 6**, representing the general information of the current validation work. Each model isolates specific aspects of the connector's mechanical response.

The simplified model FEM_SP_160_1 in Fig. 6 (a) captured the influence of initial clearances at the locking plates, reproducing slip at low load levels. The corresponding force–displacement curve can be divided into three stages: (i) *elastic friction*, (ii) *softening due to slip*, and (iii) *post-engagement tensile response*.

FEM_SP_160_2 presented in Fig. 6 (b), friction was found to play a dominant role in the connection behaviour. Increasing the friction coefficient (μ) from 0.30 to 0.50 did not affect the initial stiffness (~282.5 kN/mm) but increased the peak resistance by up to 48.5%. These findings confirm that friction increase the axial capacity of Spider connector.

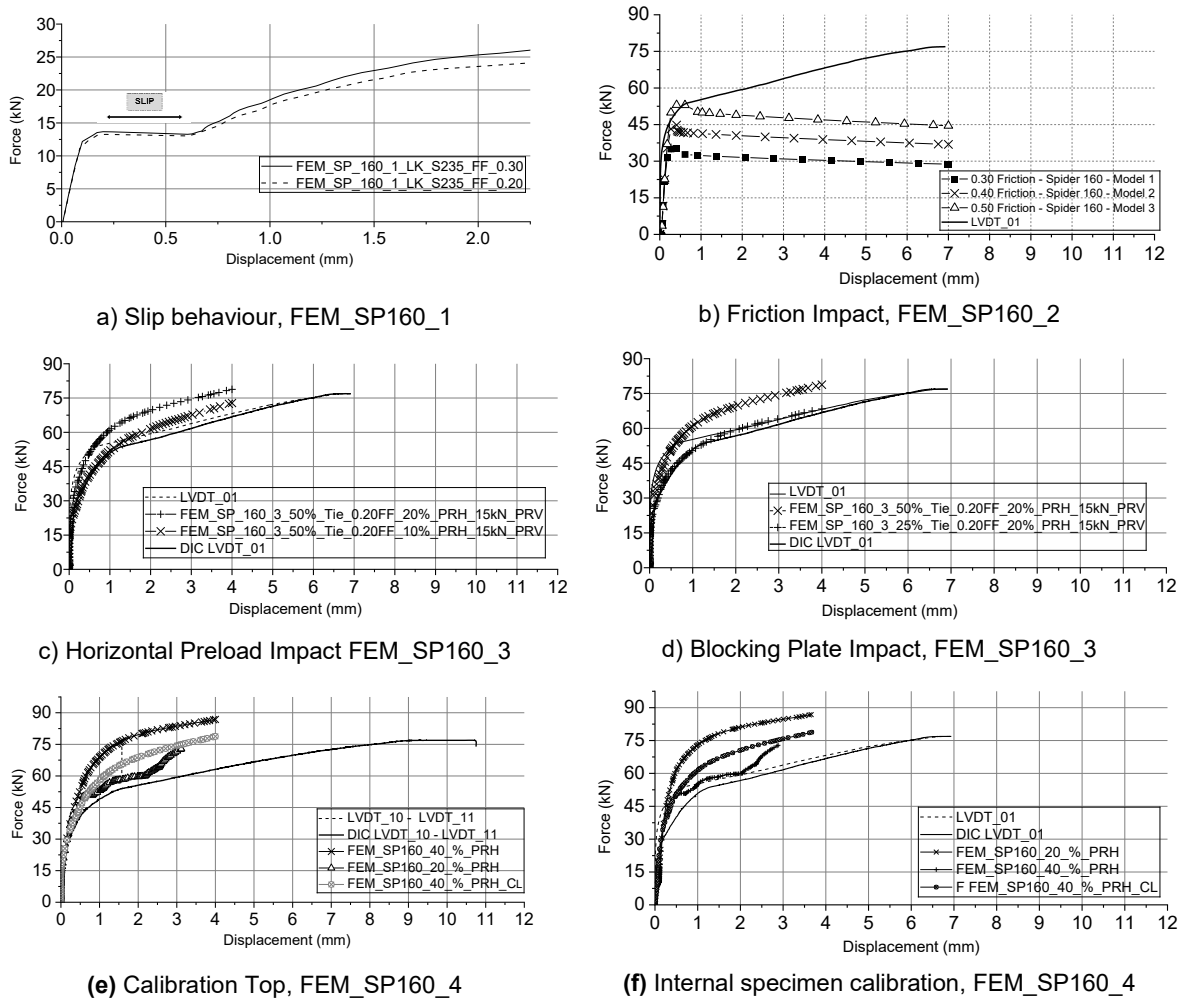

a) Slip behaviour, FEM_SP160_1

b) Friction Impact, FEM_SP160_2

c) Horizontal Preload Impact FEM_SP160_3

d) Blocking Plate Impact, FEM_SP160_3

(e) Calibration Top, FEM_SP160_4

(f) Internal specimen calibration, FEM_SP160_4

Fig. 6: Summary of result data

FEM_SP_160_3 isolates the case where the joint engages only with the bottom column specimen. In this configuration, preliminary analyses indicated that a friction factor of 0.20 provided better agreement with the experimental response and more accurately represented the realistic condition. Further analysis (see **Fig. 6c**) indicated that horizontal preload significantly enhances stiffness and strength; for instance, a 20% of bolt preload in combination with 50% tie of blocking plate shown good agreement with the experimental data. Additionally, the influence of the

support condition of blocking plate welded inside the columns was studied (see **Fig. 6d**). Representing the tie surface between both elements at 50% and 25% demonstrated that the execution quality of this weld significantly affects both stiffness and resistance.

The results of FEM_SP_160_4 are presented in **Fig. 6**e and **Fig. 4f** (Calibration against the LVDT_10 and LVDT_01)**,** incorporating the complete specimen without wedges components, providing a first robust FEM framework for validation under tensile loading. Three simulations were conducted incorporating the effect of horizontal preload in the structural model. The results showed that a preload of 20% of axial rod capacity and combined with 25% tie of the blocking plate to the tube provided the best agreement with the experimental curve presented by the LVDT_10 within the elastic range. An additional model incorporating clearance also exhibited good agreement with the experimental curve; however, the slip behaviour predicted numerically was not observed in the LVDT records (after 2 mm of displacement, an abrupt increase in connection stiffness is observed, attributable to the engagement between the M6 screw and the locking holes plates). For larger deformation levels, the DIC curve should be considered for calibration process, as LVDT_10 provided reliable data only up to 1.5 mm at the upper part of the specimen due to instrumentation limitations.

6. Conclusions

The main conclusions of this study can be summarised as follows:

1. Numerical validation: The multi-step FEM strategy successfully reproduced the axial response of the Spider 160 connector, capturing slip, post-yield engagement, and ductile behaviour consistent with experiments. Model FEM_SP_160_4 replicated the tensile response with deviations below 15% regarding the top specimen calibration, providing the first reliable numerical framework for this complex connector and opening new avenues for the study of non-conventional preload systems. Coupon test data and wedge and spring components will be included in the final FEM validation.
2. Preload sensitivity and blocking plates support condition: Horizontal preloads between 20–40% of the axial tensile rod capacity significantly influenced joint strength and stiffness, while excessive preload in the vertical M10 bolts resulted in overestimated strength. The blocking plates, particularly when assumed as pinned supports, proved essential to reproduce the experimental response owing to the lack of full welding penetration (manufacturing constraint). The most accurate configuration corresponded to a preload equal to 20% of the axial tensile rod capacity combined with pinned blocking plates and no vertical preload in the M10 bolts, which yielded close agreement with the experimental results obtained from LVDT_10 (external measurement) and LVDT_01 (internal measurement). The influence of the wedge components within the linear range remains under investigation, especially for the internal calibration.

It should be emphasised that this study is ongoing, and complete validation of the Spider connector will only be achievable once coupon tests are performed and the full set of material properties is determined. At the present stage, the work constitutes a preliminary attempt to establish calibration strategies tailored to numerical models of this complex joint.

Acknowledgments

This work was partly financed by FCT / MCTES through national funds (PIDDAC) under the R&D Unit Institute for Sustainability and Innovation in Structural Engineering (ISISE), under reference UID/04029/Institute for Sustainability and Innovation in Structural Engineering (ISISE), and under the Associate Laboratory Advanced Production and Intelligent Systems

ARISE under reference LA/P/0112/2020. This article is a result of the Innovation Pact "R2UTechnologies | modular systems" (C644876810-00000019), by "R2UTechnologies" Consortium, co-financed by NextGeneration EU, through the Incentive System "Agendas para a Inovação Empresarial" ("Agendas for Business Innovation"), within the Recovery and Resilience Plan (PRR). Dr. Conde participation was financed by UPM 'Programa Propio' grant reference EST-PDI-25-0J77JO-37-NNVVUO.

Notation

IMCs	Intermodular Connections
HDR–SMA	High Damping Rubber and Shape Memory Alloy
DIC	Digital Image Correlation
LVDT	Linear Variable Differential Transformer
LK	Locking Plates (rectangular plate components of the Spider connector)
BK	Blocking Plate (welded plate inside HSS 160 × 10 columns)
PRH	Horizontal preload applied to Spider's arms
PRV	Vertical preload applied to Spider's arms
FF	Friction Factor used for contact interfaces
FEM_SP160_1	Simplified FEM model to study the impact of preload and clearances on the tensile response of the Spider connector.
FEM_SP160_2	FEM model to analyse the tensile response of the Spider connector considering friction conditions.
FEM_SP160_3	FEM model to evaluate the influence of the blocking plate and preload effects.

Reference

[1] A. W. Lacey, W. Chen, H. Hao, and K. Bi, "Review of bolted inter-module connections in modular steel buildings," May 01, 2019, *Elsevier Ltd*. doi: 10.1016/j.jobe.2019.01.035.

[2] X. Liu, C. Hou, J. Peng, Y. Wang, and K. J. R. Rasmussen, "Recent advancements of inter-module connections for modular buildings: An overview and multi-dimensional assessment," *Eng Struct*, vol. 335, Jul. 2025, doi: 10.1016/j.engstruct.2025.120378.

[3] C. Dan-Adrian and K. D. Tsavdaridis, "A comprehensive review and classification of inter-module connections for hot-rolled steel modular building systems," *Journal of Building Engineering*, vol. 50, Jun. 2022, doi: 10.1016/j.jobe.2022.104006.

[4] S. Srisangeerthanan, M. J. Hashemi, P. Rajeev, E. Gad, and S. Fernando, "Review of performance requirements for inter-module connections in multi-story modular buildings," Mar. 01, 2020, *Elsevier Ltd*. doi: 10.1016/j.jobe.2019.101087.

[5] G. Nadeem, N. A. Safiee, N. A. Bakar, I. A. Karim, and N. A. M. Nasir, "Connection design in modular steel construction: A review," Oct. 01, 2021, *Elsevier Ltd*. doi: 10.1016/j.istruc.2021.06.060.

[6] C. D. Annan, M. A. Youssef, and M. H. El Naggar, "Seismic vulnerability assessment of modular steel buildings," Journal of Earthquake Engineering," *Journal of Earthquake Engineering,* vol. 13, no. 8, pp. 1065–1088, 2009.

[7] T. Gunawardena, T. Ngo, P. Mendis, and J. Alfano, "Innovative Flexible Structural System Using Prefabricated Modules," The University of Melbourne, 2016.

[8] B. Hajimohammadi, S. Das, H. Ghaednia, and J. Dhanapal, "Structural performance of registration pin connection in VectorBloc modular construction system," *J Constr Steel Res*, vol. 197, Oct. 2022, doi: 10.1016/j.jcsr.2022.107464.

[9] K. Lee, K. J. R. Rasmussen, and B. H. Cho, "Bolt-free post-tensioned connection for steel-framed modular buildings and design for optimal preloading," *J Constr Steel Res*, vol. 218, Jul. 2024, doi: 10.1016/j.jcsr.2024.108703.

[10] A. W. Lacey, W. Chen, H. Hao, and K. Bi, "Effect of inter-module connection stiffness on structural response of a modular steel building subjected to wind and earthquake load," *Eng Struct*, vol. 213, Jun. 2020, doi: 10.1016/j.engstruct.2020.110628.

[11] D. H. Shin and H. J. Kim, "Load-Carrying Mechanism of Post-Tensioned Inter-Module Connections Implemented into Modular Steel Buildings," *Journal of Earthquake Engineering*, vol. 27, no. 4, pp. 898–928, 2023, doi: 10.1080/13632469.2022.2033358.

[12] D. A. Corfar and K. D. Tsavdaridis, "A hybrid inter-module connection for steel modular building systems with SMA and high-damping rubber components," *Eng Struct*, vol. 289, Aug. 2023, doi: 10.1016/j.engstruct.2023.116281.

[13] H. Rajanayagam *et al.*, "Effect of design variation in behaviour and performance of End-plate-Type intermodular connection," *Structures*, vol. 56, Oct. 2023, doi: 10.1016/j.istruc.2023.104899.

[14] M. Kujawa, Smakosz, P. Iwicki, A. Perliński, and J. Tejchman, "Mechanical performance investigations of a post-tensioned inter-module connection in steel buildings," *Structures*, vol. 71, Jan. 2025, doi: 10.1016/j.istruc.2025.108187.

[15] J. Peng, C. Hou, and L. Shen, "Lateral resistance of multi-story modular buildings using tenon-connected inter-module connections," *J Constr Steel Res*, vol. 177, Feb. 2021, doi: 10.1016/j.jcsr.2020.106453.

[16] Y. S. Chua, J. Y. R. Liew, and S. D. Pang, "Modelling of connections and lateral behavior of high-rise modular steel buildings," *J Constr Steel Res*, vol. 166, Mar. 2020, doi: 10.1016/j.jcsr.2019.105901.

[17] L. A. Proença Simões da Silva, D. Gomes Andrade, T. Sabari Shunmuga, J. Conde Conde, F. Ljubinković, and A. F. Henriques Parente dos Santos, "Connection system for modular construction of multi-storey buildings," Patent WO 2024/224161 A1, World Intellectual Property Organization, Oct. 31, 2024.

[18] L. A. Proença Simões da Silva, D. Gomes Andrade, S. Shunmugam, J. Conde Conde, F. Ljubinković, and A. F. Henriques Parente dos Santos, "3D connector for modular construction of multi-story buildings," Patent WO 2024/224160 A1, World Intellectual Property Organization, Oct. 31, 2024.

[19] X. Yun and L. Gardner, "Stress-strain curves for hot-rolled steels," *J Constr Steel Res*, vol. 133, pp. 36–46, Jun. 2017, doi: 10.1016/j.jcsr.2017.01.024.